

DIRECTION ESTIMATION OF CORRELATED/COHERENT SIGNALS BY SPARSELY REPRESENTING THE SIGNAL-SUBSPACE EIGENVECTORS

Zhi-Chao Sha^{*}, Zhang-Meng Liu, Zhi-Tao Huang, and Yi-Yu Zhou

College of Electronic Science and Engineering, National University of Defense Technology, Changsha, Hunan, 410073, P. R. China

Abstract—This paper addresses the problem of direction-of-arrival (DOA) estimation of correlated and coherent signals, and two sparsity-inducing methods are proposed. In the first method named L1-EVD, the signal-subspace eigenvectors are represented jointly with well-chosen hard thresholds attached to the representation residue of each eigenvector. Then only the eigenvector corresponding to the largest eigenvalue is reserved for DOA estimation via sparse representation, which aims at highly correlated signals, and a method named L1-TEVD (TEVD: Truncated EVD) is proposed. Simulation results show that L1-EVD and L1-TEVD both surpass L1-SVD in DOA estimation performance and computation efficiency for highly correlated and coherent signals.

1. INTRODUCTION

Direction-of-arrival (DOA) estimation techniques have been frequently used in many applications involving electromagnetic, acoustic, seismic sensing, etc. [1–5]. When the incident signals are highly correlated or coherent, the performance of conventional high-resolution DOA estimation methods [6–10] will deteriorate significantly [11]. Spatial smoothing [12] provides a way to make up for such drawback in those methods, but it adapts only to arrays with special geometries and sacrifices some array aperture.

The recently interest-attracting technique of sparse representation provides a new perspective for DOA estimation [13]. The sparsity-inducing methods seek a trade-off between minimal fitting error of the

Received 9 April 2013, Accepted 8 May 2013, Scheduled 21 May 2013

* Corresponding author: Zhi-Chao Sha (shazhichao.163@163.com).

data and model parsimony, and they succeed to detect the incident signal number and estimate their directions simultaneously.

Several sparsity-inducing DOA estimation methods have been proposed in the past decade. The first estimator, as far as we know, is the Global Matched Filter (GMF) of Fuchs that bases on the beamspace samples [14], but it only adapts to uniform circular arrays. Malioutov et al. then proposed the method of L1-SVD to address the general DOA estimation problem [15]. L1-SVD first decomposes the array output and extracts the signal energy into K (the signal number) singular-vectors, and then represents them under sparsity constraint to estimate the signal directions. L1-SVD contributes much to the development of the sparsity-inducing DOA estimation techniques, and it also adapts well to signal correlation. For correlated signals, although the borderline between the signal- and noise-subspaces becomes vague, most of the signal energy is still contained in the signal-subspace eigenvectors, so L1-SVD shows satisfying adaptation to signal correlation [15, 16]. More recently, Hyder and Mahata introduced their joint sparsity-enforcing technique to DOA estimation, and proposed the method of JLZA-DOA [17]. JLZA-DOA uses a family of Gaussian functions to approach the canonical but NP hard ℓ_0 -norm sparsity penalty, but as the Gaussian parameters are tune subjectively, the method is not guaranteed to global convergence [18]. Zhang et al. cast the problem of localization of narrow band sources in the presence of mutual coupling into the framework of sparse solution finding. The proposed alternating minimization technique is applicable for noise free covariance matrix as well as the observation data, where single snapshot and multiple snapshots can both be used [19]. But its computational cost is very high due to the dimension of its model.

In this paper, we address the problem of DOA estimation for multiple correlated or coherent signals, and two methods, named L1-EVD and L1-TEVD (TEVD: Truncated EVD), will be proposed. Those two methods realize DOA estimation by sparsely representing all the eigenvectors within the signal-subspace, or just the eigenvector corresponding to the largest eigenvalue. The essential character that distinguishes L1-EVD and L1-TEVD from L1-SVD is that the former two ground on the eigenvectors with unattached thresholds, while the latter one grounds on the singular-vectors with associated threshold. Such difference helps L1-EVD and L1-TEVD to surpass L1-SVD in DOA estimation of highly correlated and coherent signals, with the reason given in Sections 2 and 3, and verified in Section 4. L1-TEVD is just a simplified version of L1-EVD by retaining only the eigenvector corresponding to the largest eigenvalue, aiming at the application to

highly correlated and adjacent signals. The simplification is validated as this eigenvector contains most signal energy when the correlation is significant.

The rest of this paper mainly consists of four parts. Section 2 reviews the array output model and existing DOA estimation methods. Section 3 presents the methods of L1-EVD and L1-TEVD. Section 4 carries out simulations to demonstrate the performance of the newly proposed methods. Section 5 concludes the whole paper.

2. PROBLEM FORMULATION

Suppose that K narrowband Gaussian signals impinge onto an M -element array from directions of $\theta_1, \dots, \theta_K$, respectively, N snapshots are collected by the array receiver, and the snapshot at the n th time instant is given by

$$\mathbf{x}(n) = \mathbf{A}(\boldsymbol{\theta}) \mathbf{s}(n) + \mathbf{v}(n), \quad (1)$$

where $\boldsymbol{\theta} = [\theta_1, \dots, \theta_K]$, $\mathbf{A}(\boldsymbol{\theta}) = [\mathbf{a}(\theta_1), \dots, \mathbf{a}(\theta_K)]$ is the responding matrix of the K signals, $\mathbf{s}(n)$ is the signal waveform, and $\mathbf{v}(n)$ is the additive noise with variance σ_v^2 .

To obtain the signal directions from $\mathbf{X} = [\mathbf{x}(1), \dots, \mathbf{x}(N)]$, conventional subspace based methods [9] first estimate the covariance matrix as follows,

$$\hat{\mathbf{R}} = \frac{1}{N} \mathbf{X} \mathbf{X}^H, \quad (2)$$

and then eigen-decompose it to estimate the signal-subspace $\hat{\mathbf{U}}_s$ and noise-subspace $\hat{\mathbf{U}}_v$,

$$\hat{\mathbf{R}} = [\hat{\mathbf{U}}_s \quad \hat{\mathbf{U}}_v] \hat{\boldsymbol{\Lambda}} [\hat{\mathbf{U}}_s \quad \hat{\mathbf{U}}_v]^H, \quad (3)$$

where $\hat{\boldsymbol{\Lambda}}$ is a diagonal matrix with the M degressive eigenvalues on its diagonal. Finally, an orthogonality-testing process between the array manifold and noise-subspace is carried out for DOA estimation,

$$\hat{\boldsymbol{\theta}} = \arg \max_{\boldsymbol{\theta}} \frac{1}{\|\mathbf{a}^H(\boldsymbol{\theta}) \hat{\mathbf{U}}_v\|_2^2}. \quad (4)$$

If the incident signals are highly correlated or completely coherent, the noise-subspace estimate may be biased, and the DOA estimates derived from (4) deteriorate in precision.

Sparsity-inducing methods estimate the signal directions by representing the observation under sparsity constraint. Take L1-SVD [15] for example, it first decomposes the array output to extract

the signal information,

$$\mathbf{X} = \mathbf{W}_1 \mathbf{\Sigma} \mathbf{W}_2^H, \quad (5)$$

where \mathbf{W}_1 and \mathbf{W}_2 are the left and right singular matrices, and $\mathbf{\Sigma}$ is a diagonal matrix consisting of the singular-values. If the incident signal number is assumed known, the first K singular-vectors in (5) (i.e., the signal-subspace) are retained to form a new observation matrix \mathbf{Y} ,

$$\mathbf{Y} = \mathbf{X} \mathbf{W}_2 \mathbf{D}_K \triangleq [\mathbf{y}_1, \dots, \mathbf{y}_K], \quad (6)$$

where $\mathbf{D}_K = \begin{bmatrix} \mathbf{I}_K \\ 0 \end{bmatrix}^H$. In this procedure, the singular-vectors are weighted according to the singular-values.

Then an overcomplete spatial dictionary $\bar{\mathbf{A}} = [\{\mathbf{a}(\theta)\}_{\theta \in \Theta}]$ is formed on the possible signal direction set Θ , under the assumption that each vector in \mathbf{Y} is a noisy weighted sum of only a few atoms in $\bar{\mathbf{A}}$, i.e., $\mathbf{y}_k = \bar{\mathbf{A}} \bar{\mathbf{s}}(k) + \mathbf{v}_y(k)$, where $\bar{\mathbf{s}}(k)$ owns non-zero values only at indexes corresponding to the signal directions, and $\mathbf{v}_y(k)$ is the representation residue. Based on the spatially overcomplete formulation of \mathbf{Y} , one can solve the following BPDN (Basis Pursuit DeNoising) problem [20] for DOA estimation,

$$(\text{L1-SVD}) \quad \min \|\mathbf{Y} - \bar{\mathbf{A}} \bar{\mathbf{S}}\|_F^2 + \tau \left\| \bar{\mathbf{s}}^{(\ell_2)} \right\|_1, \quad (7)$$

where τ is the regularization factor, $\bar{\mathbf{S}} = [\bar{\mathbf{s}}(1), \dots, \bar{\mathbf{s}}(K)]$, and $\bar{\mathbf{s}}^{(\ell_2)} = [\bar{\mathbf{s}}_{\theta}^{(\ell_2)}]_{\theta \in \Theta}$, $\bar{\mathbf{s}}_{\theta}^{(\ell_2)} = \|\bar{\mathbf{s}}_{\theta}(1), \dots, \bar{\mathbf{s}}_{\theta}(K)\|_2$, with $\bar{\mathbf{s}}_{\theta}(k)$ being the value of $\bar{\mathbf{s}}(k)$ at direction θ . The symbol $\|\cdot\|_1$ denotes the ℓ_1 norm of a vector, and $\|\cdot\|_F$ denotes the Frobenius norm of a matrix. The above objective function can also be rewritten in the following constrained form [21],

$$\min \left\| \bar{\mathbf{s}}^{(\ell_2)} \right\|_1, \quad \text{subject to } \|\mathbf{Y} - \bar{\mathbf{A}} \bar{\mathbf{S}}\|_F^2 \leq \xi, \quad (8)$$

where ξ is the fitting-error threshold between \mathbf{Y} and the representation model $\bar{\mathbf{A}} \bar{\mathbf{S}}$.

As the snapshots are limited in practical applications, the singular-vector estimates are not completely accurate and show different estimation precision, and the optimality of the observation matrix obtained following (6) is not guaranteed. Malioutov himself also discovered that weighting the singular-vectors with the eigenvalues instead of the singular-values helped to improve the performance of L1-SVD [13]. However, both those two groups of weighting factors are selected empirically, and no theoretical result is available to support such selection. In addition, a particular regularization factor τ_k can be determined for each \mathbf{y}_k according to the L-curve criterion [22]. But

as different singular-vectors are of different energy and precision, the optimal τ_k 's for them are probably different, so there is a trade-off between those τ_k 's when choosing overall τ in (7). If the incident signals are spatially much adjacent and temporally highly correlated, the energy and precision diversities between different singular-vectors is much more significant, which makes optimal tuning of the free parameters even more difficult and leads to performance deterioration when using the jointly penalized objective functions of (7) and (8).

3. L1-EVD AND L1-TEVD METHODS

In order to avoid the trade-off during regularization factor selection in L1-SVD, and inheriting the superiority of the sparsity-inducing methods over conventional ones at the same time, we turn to the idea of sparsely representing the eigenvectors for DOA estimation. In-depth eigen-analysis will be carried out to select fitting-error thresholds for each eigenvector, resulting in a method named L1-EVD. When the incident signals are highly correlated and spatially adjacent, the energy of the array output will flock together in a subspace of only one dimension of the incident signals, thus we only retain and represent the eigenvector corresponding to the largest eigenvalue for DOA estimation, resulting in the method of L1-TEVD (TEVD: Truncated EVD).

3.1. L1-EVD

If no perturbation error is contaminated in the covariance matrix estimate $\hat{\mathbf{R}}$, the signal-subspace estimate \mathbf{U}_s is a linear transformation of the responding matrix of the incident signals, i.e.,

$$\mathbf{U}_s = \mathbf{A}(\boldsymbol{\theta}) \mathbf{Q}, \quad (9)$$

where \mathbf{Q} is the reformulation matrix. Denote the k th eigenvector (corresponding to the k th largest eigenvalue as default) by \mathbf{u}_k , the k th column of \mathbf{Q} by \mathbf{q}_k , then the following equality holds,

$$\mathbf{u}_k = \mathbf{A}(\boldsymbol{\theta}) \mathbf{q}_k. \quad (10)$$

Thus \mathbf{u}_k also has a sparse representation on $\bar{\mathbf{A}}$, i.e., $\mathbf{u}_k = \bar{\mathbf{A}}\bar{\mathbf{q}}_k$, where $\bar{\mathbf{q}}_k$ has non-zero values only at indexes corresponding to the signal directions. In practice, the signal-subspace estimate is perturbation-contaminated due to limited snapshots, which is denoted by

$$\hat{\mathbf{u}}_k = \bar{\mathbf{A}}\bar{\mathbf{q}}_k + \boldsymbol{\varepsilon}_k. \quad (11)$$

In this paper, we use the BPDN model to sparsely representing the $\hat{\mathbf{u}}_k$'s for DOA estimation, and the fitting-error constrained objective

function for each eigenvector is

$$\min \|\bar{\mathbf{q}}_k\|_0 \quad \text{subject to} \quad \|\hat{\mathbf{u}}_k - \bar{\mathbf{A}}\bar{\mathbf{q}}_k\|_2 \leq \beta_k, \quad (12)$$

where β_k is the fitting-error threshold that depends on the variance of $\boldsymbol{\varepsilon}_k$.

Solving (12) straightforwardly is a NP-hard problem [23], and the ℓ_0 -norm can be approximated by the ℓ_1 -norm to make the objective function convex and globally convergent, thus (12) is transformed to the following form,

$$\min \|\bar{\mathbf{q}}_k\|_1 \quad \text{subject to} \quad \|\hat{\mathbf{u}}_k - \bar{\mathbf{A}}\bar{\mathbf{q}}_k\|_2 \leq \beta_k. \quad (13)$$

In order to make sufficient use of the signal energy contained in the signal-subspace, all the K eigenvectors should be represented jointly, which can be realized with joint $\ell_{2,1}$ -norm function, thus resulting in the objective function of L1-EVD, i.e.,

$$\begin{aligned} \text{(L1-EVD)} \quad & \min \|\bar{\mathbf{q}}\|_1 \quad \text{subject to} \quad \bar{\mathbf{q}}(\theta) \geq \|\bar{\mathbf{q}}_1(\theta), \dots, \bar{\mathbf{q}}_K(\theta)\|_2, \\ & \text{and} \quad \|\hat{\mathbf{u}}_k - \bar{\mathbf{A}}\bar{\mathbf{q}}_k\|_2 \leq \beta_k, k = 1, \dots, K, \end{aligned} \quad (14)$$

where $\bar{\mathbf{q}}_k(\theta)$ is the value of $\bar{\mathbf{q}}_k$ at direction θ , and the first constraint is introduced to force joint sparsity on the representations of different eigenvectors. In (14), unattached thresholds are set for the fitting error of the K eigenvectors separately, thus evading possible performance deterioration during the selection of trade-off regularization factor in L1-SVD. The locations of the non-zero values in the solution to (14), denoted by $\hat{\mathbf{q}}$, corresponds to the signal directions. The performance of the solution to L1-EVD depends heavily on the optimization of the thresholds β_1, \dots, β_K . We carry out an in-depth analysis on the eigenvector perturbation for the threshold selection in the following subsection.

3.2. Fitting-error Threshold Selection

Denote the estimation error of the covariance matrix by $\tilde{\mathbf{R}} = \hat{\mathbf{R}} - \mathbf{R}$, and make a first-order approximation of the eigenvectors before normalization as follows [24],

$$\tilde{\mathbf{u}}_i \simeq \mathbf{u}_i + \sum_{\substack{m=1 \\ m \neq i}}^M c_{i,m} \mathbf{u}_m, \quad i = 1, \dots, M. \quad (15)$$

Eq. (15) holds because the vector set $[\mathbf{u}_1, \dots, \mathbf{u}_M]$ spans the whole space of \mathbb{C}^M . Straightforward derivations can be carried out to conclude that [24],

$$c_{i,m} = \frac{\mathbf{u}_m^H \tilde{\mathbf{R}} \mathbf{u}_i}{\lambda_m - \lambda_i}, \quad m \neq i, \quad (16)$$

where λ_m is the m th largest eigenvalue of \mathbf{R} . Eq. (16) indicates that $|c_{i,m}| \ll 1$ when the number of snapshots is adequate. Then the i th eigenvector $\hat{\mathbf{u}}_i$ can be derived by normalizing $\check{\mathbf{u}}_i$, which is approximately given as follows by neglecting the higher-than-second-order terms,

$$\hat{\mathbf{u}}_i = \left(\|\check{\mathbf{u}}_i\|_2 \right)^{-1} \check{\mathbf{u}}_i \simeq \left(1 - \frac{1}{2} \sum_{\substack{m=1 \\ m \neq i}}^M |c_{i,m}|^2 \right) \left(\mathbf{u}_i + \sum_{\substack{m=1 \\ m \neq i}}^M c_{i,m} \mathbf{u}_m \right). \quad (17)$$

Equation (17) shows that each eigenvector estimate is a weighted sum of all the M perturbation-free eigenvectors. As the first K eigenvectors are contained in the signal-subspace, only the dispersion from the noise-subspace eigenvectors contributes to the representation error of them. Denote the deviation of the k th ($k = 1, \dots, K$) eigenvector from the observation model $\bar{\mathbf{A}}\bar{\mathbf{q}}$ by $\boldsymbol{\varepsilon}_k$, it can be expressed as follows approximately by keeping only the first-order terms,

$$\boldsymbol{\varepsilon}_k \simeq \sum_{m=K+1}^M c_{k,m} \mathbf{u}_m, \quad k = 1, \dots, K. \quad (18)$$

The variance of $\boldsymbol{\varepsilon}_k$ is

$$\|\boldsymbol{\varepsilon}_k\|_2^2 \simeq \sum_{m=K+1}^M |c_{k,m}|^2 \simeq \sum_{m=K+1}^M \frac{(\mathbf{u}_m^H \tilde{\mathbf{R}} \mathbf{u}_k) (\mathbf{u}_k^H \tilde{\mathbf{R}} \mathbf{u}_m)}{(\lambda_k - \lambda_m)^2}, \quad k = 1, \dots, K. \quad (19)$$

For $k \in \{1, \dots, K\}$ and $m \in \{K+1, \dots, M\}$, the following equality holds,

$$\mathbf{u}_m^H \tilde{\mathbf{R}} \mathbf{u}_k = \mathbf{u}_m^H \hat{\mathbf{R}} \mathbf{u}_k = \frac{1}{N} \sum_{n=1}^N \mathbf{u}_m^H \mathbf{x}(n) \mathbf{x}^H(n) \mathbf{u}_k. \quad (20)$$

When N is adequately large, $\mathbf{u}_m^H \tilde{\mathbf{R}} \mathbf{u}_k$ is approximately Gaussian distributed according to the law of large numbers. Moreover, as $\lambda_{K+1} = \dots = \lambda_M = \sigma_v^2$ and the noise-subspace eigenvectors are identically correlated with the additive noise, one can conclude that $\mathbf{u}_{m_1}^H \tilde{\mathbf{R}} \mathbf{u}_k$ and $\mathbf{u}_{m_2}^H \tilde{\mathbf{R}} \mathbf{u}_k$ have equal variances for $m_1 \neq m_2$, and $k \in \{1, \dots, K\}$, $m_1, m_2 \in \{K+1, \dots, M\}$. Denote the variance of $\mathbf{u}_m^H \tilde{\mathbf{R}} \mathbf{u}_k$ for all $m \in \{K+1, \dots, M\}$ by γ_k^2 , then $\frac{(\lambda_k - \sigma_v^2)^2}{\gamma_k^2} \|\boldsymbol{\varepsilon}_k\|_2^2$ is χ^2 -distributed with freedom $M - K$.

The distribution of $\|\boldsymbol{\varepsilon}_k\|_2^2$ should be exploited during threshold-selection in (14) to guarantee a certain detection probability. Define

$\mu_k = \frac{(\lambda_k - \sigma_v^2)^2}{\gamma_k^2} \|\boldsymbol{\varepsilon}_k\|_2^2 \sim \chi^2(M - K)$, then we should set $\mu_k \leq \mu_k(\alpha) = \chi_\alpha^2(M - K)$ (the upper α fractile of $\chi^2(M - K)$) to decrease the false detection probability to a very low level of α , such as 0.01. The corresponding constraint threshold for $\|\boldsymbol{\varepsilon}_k\|_2^2$ is

$$\|\boldsymbol{\varepsilon}_k\|_2^2 \leq \frac{\gamma_k^2}{(\lambda_k - \sigma_v^2)^2} \chi_\alpha^2(M - K). \quad (21)$$

The final determination of the above threshold requires the value of the variance γ_k^2 . We give two lemmas first for the calculation of it in the following.

Lemma 1: Assume that the incident signals and additive noise are zero-mean and independent Gaussian processes, and denote the estimation error of the covariance matrix by $\tilde{\mathbf{R}}$, then it holds that [25],

$$E(\tilde{\mathbf{R}}_{ik} \tilde{\mathbf{R}}_{lm}) = \frac{1}{N} \mathbf{R}_{im} \mathbf{R}_{lk}, \quad (22)$$

where $E(\cdot)$ stands for the expectation of a random variable, $\tilde{\mathbf{R}}_{ik}$ and \mathbf{R}_{ik} are the (i, k) th element of $\tilde{\mathbf{R}}$ and \mathbf{R} , respectively.

Lemma 2: Under the same assumption as Lemma 1, the following equality holds for $\tilde{\mathbf{R}}$ and four randomly chosen $M \times 1$ vectors $\boldsymbol{\alpha}_1, \boldsymbol{\alpha}_2, \boldsymbol{\alpha}_3, \boldsymbol{\alpha}_4$ [25],

$$E\left[\left(\boldsymbol{\alpha}_1^H \tilde{\mathbf{R}} \boldsymbol{\alpha}_2\right) \left(\boldsymbol{\alpha}_3^H \tilde{\mathbf{R}} \boldsymbol{\alpha}_4\right)\right] = \frac{1}{N} \left(\boldsymbol{\alpha}_1^H \mathbf{R} \boldsymbol{\alpha}_4\right) \left(\boldsymbol{\alpha}_3^H \mathbf{R} \boldsymbol{\alpha}_2\right).$$

Lemma 1 and 2 are given in [25] as exercises. In the Appendix, we provide a brief proof for Lemma 1, and Lemma 2 can be concluded with further straightforward derivation.

Based on Lemma 2, the variance γ_k^2 can be calculated as follows,

$$\gamma_k^2 = E\left[\left(\mathbf{u}_m^H \tilde{\mathbf{R}} \mathbf{u}_k\right) \left(\mathbf{u}_m^H \tilde{\mathbf{R}} \mathbf{u}_k\right)^H\right] = \frac{1}{N} \left(\mathbf{u}_m^H \mathbf{R} \mathbf{u}_m\right) \left(\mathbf{u}_k^H \mathbf{R} \mathbf{u}_k\right) = \frac{\lambda_k \sigma_v^2}{N},$$

$$m \in \{K + 1, \dots, M\}. \quad (23)$$

Substituting (23) into (21) yields a mathematically tractable constraint for the eigenvector perturbations,

$$\|\boldsymbol{\varepsilon}_k\|_2^2 \leq \frac{\lambda_k \sigma_v^2}{N (\lambda_k - \sigma_v^2)^2} \chi_\alpha^2(M - K) \triangleq \beta_k^2, \quad k \in \{1, \dots, K\}. \quad (24)$$

Hence, the fitting-error thresholds in (14) can be derived from (24) as

$$\beta_k \leq \left[\frac{\lambda_k \sigma_v^2}{N (\lambda_k - \sigma_v^2)^2} \chi_\alpha^2(M - K) \right]^{\frac{1}{2}}, \quad k \in \{1, \dots, K\}. \quad (25)$$

In practical applications, λ_k ($k = 1, \dots, K$) can be approximated by $\hat{\lambda}_k$ ($k = 1, \dots, K$), and σ_v^2 can be approximated by $\frac{1}{M-K} \sum_{m=K+1}^M \hat{\lambda}_m$ in (25) to calculate β_k for different k . Finally, those thresholds are substituted in (14) to form the L1-EVD objective function and estimate $\bar{\mathbf{q}}$. Many computational methods are available for solving (14) [26], and we choose the toolbox of SeDuMi to realize this process for convenience.

3.3. L1-TEVD

As the DOA estimation of well-separated sources has been solved by existing methods perfectly, we mainly focus on the scenarios of spatially adjacent and temporally correlated signals in this paper. Under such settings, the eigenvalues obtained from (3) attenuates rapidly, thus the first eigenvector contains most of the signal energy. The perturbation variance of the eigenvectors given in (24) also indicates that the precision of the eigenvector estimates deteriorates synchronously. Therefore, simple abnegation of the second to K th eigenvectors will not loss much signal energy. Contrarily, obvious improvements in at least three aspects can be gained from such abnegation when compared to L1-SVD. First, the reconstruction model of (14) can be greatly simplified, thus saving much computation load. Second, no weighting vector is required for multiple eigenvectors. Last, the selection of the threshold becomes more convenient.

Bases on those superiorities derived from such abnegation, we propose a simplified version of L1-EVD, named L1-TEVD, as follows,

$$\text{(L1-TEVD)} \quad \min \|\bar{\mathbf{q}}_1\|_1 \quad \text{subject to} \quad \|\hat{\mathbf{u}}_1 - \bar{\mathbf{A}}\bar{\mathbf{q}}_1\|_2 \leq \beta_1, \quad (26)$$

where the threshold β_1 is given by (25), and the toolbox of SeDuMi is used to solve (26).

The validation of using L1-TEVD for DOA estimation depends on various factors, including the angular distance and correlation degree between the incident signals, we leave the analysis to the following section via simulations.

4. SIMULATION RESULTS

In this section, we carry out simulations to demonstrate the performance of L1-EVD and L1-TEVD in various scenarios, and compare them with existing methods.

Suppose that two equal-power signals impinge onto an 8-element uniform linear array (ULA) simultaneously, and the ULA is inter-spaced by half-wavelength. The $[-90^\circ \ 90^\circ]$ space is divided into

1° intervals when forming the dictionary $\bar{\mathbf{A}}$ (further grid refinement procedure [15] can be introduced to improve the estimation precision). The upper fractile of the χ^2 distribution is set to $\alpha = 0.01$ when calculating the thresholds for L1-EVD and L1-TEVD with (25). The additive noise is zero-mean and independent Gaussian process. The performance of different methods in DOA estimation is compared according to the ability of resolving adjacent signals, and successful resolution is defined when the two most significant spectrum peaks locate near the true signal directions, with biases no larger than 2° . Actually, this criterion compares the methods' performance in both model reconstruction and DOA estimation precision synthetically.

4.1. Solving Signals with Different Correlation Coefficients

Fix the signal-to-noise ratio (SNR) of both signals at -5 dB, their directions at 10° and 17° , the snapshot number at 100, and vary the correlation coefficient of the two signals from 0 to 1.

For each correlation coefficient, 1000 trials are carried out, and the probabilities of successful resolution of MUSIC, L1-SVD, L1-EVD and L1-TEVD are given in Fig. 1.

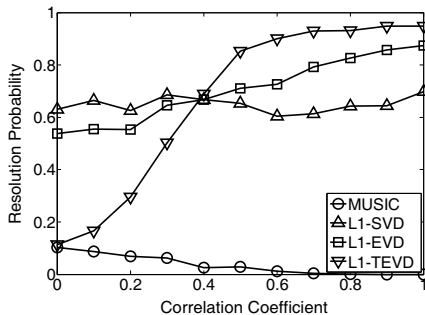


Figure 1. Resolution probabilities of MUSIC, L1-SVD, L1-EVD and L1-TEVD when correlation coefficient increases.

Figure 1 shows that MUSIC fails to efficiently separate the two signals and that its resolution probability decreases from 10% to 0 when the correlation coefficient increases. Among the three sparsity-inducing methods, L1-SVD obtains the highest resolution probability when the correlation coefficient is lower than 0.4, while L1-EVD is slightly worse, and L1-TEVD performs worst. That is because when the two signals are weakly correlated, the second signal-subspace eigenvector still contains much signal energy, thus simply abnegating it induces significant SNR loss. As the correlation between the two signals strengthens, the signal energy contained in the second

eigenvector attenuates gradually. When the correlation coefficient is larger than 0.4, both L1-EVD and L1-TEVD surpass L1-SVD in resolution probability, and L1-TEVD performs the best. The above phenomenon indicates that the newly proposed methods are more adaptable to correlated signals than existing methods. Moreover, the average CPU time of the three sparsity-inducing methods in completing a single trial is listed in Table 1, which indicates that L1-EVD and L1-TEVD are computationally more efficient than L1-SVD.

Table 1. Average CPU time of the sparsity-inducing methods.

Method	L1-SVD	L1-EVD	L1-TEVD
CPU time (sec)	0.284	0.231	0.169

The performance and computation analysis in Fig. 1 and Table 1 demonstrates that L1-EVD and L1-TEVD are well designed for DOA estimation of highly correlated and coherent signals, and L1-TEVD shows more significant superiority over its counterparts in both resolution ability and computational efficiency.

4.2. Solving Signals with Different Angular Distances

Fix the SNR of both signals at -5 dB, the snapshot number at 100, the correlation coefficient of the two signals at 0.7, the direction of the first signal at 10° , and vary the direction of the second signal from 14° to 22° (i.e., the angular distance increases from 4° to 12°). At each angular distance, 1000 trials are carried out, and the probabilities of successful resolution of MUSIC, L1-SVD, L1-EVD and L1-TEVD are given in Fig. 2.

As the two signals are highly correlated, MUSIC performs much worse than those sparsity-inducing methods, among which L1-TEVD gains the highest resolution probability, and L1-EVD also outperforms L1-SVD by some degree. This result is identical to that given in Fig. 1 at the correlation coefficient value of 0.7.

4.3. Solving Signals with Different SNR

Fix the directions of the two incident signals at 10° and 17° , respectively, the correlation coefficient at 0.7, the snapshot number at 100, and vary the SNR of each signal from -15 dB to 5 dB. At each SNR value, 1000 trials are carried out, and the probabilities of successful resolution of MUSIC, L1-SVD, L1-EVD and L1-TEVD are given in Fig. 3.

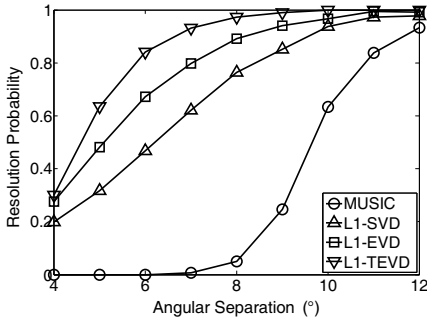


Figure 2. Resolution probabilities of MUSIC, L1-SVD, L1-EVD and L1-TEVD when angular distance increases.

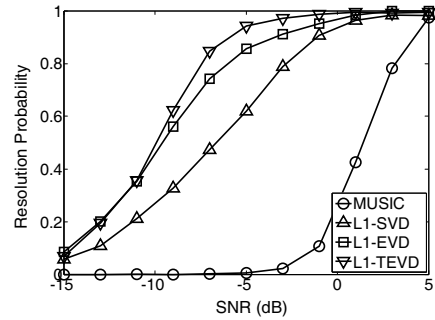


Figure 3. Resolution probabilities of MUSIC, L1-SVD, L1-EVD and L1-TEVD when SNR increases.

Figure 3 shows that MUSIC fails completely when the signal SNR is lower than -5 dB, and L1-EVD and L1-TEVD outperform L1-SVD for all the SNR values, with L1-TEVD achieving the highest resolution probability among them in most cases.

4.4. Solving Signals with Different Snapshots

Fix the directions of the two incident signals at 10° and 17° , respectively, their SNR at -5 dB, the correlation coefficient at 0.7, and increase the snapshot number from 20 to 200. At each snapshot number, 1000 trials are carried out, and the probabilities of successful resolution of MUSIC, L1-SVD, L1-EVD and L1-TEVD are given in Fig. 4.

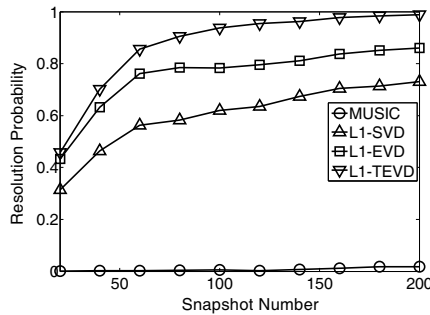


Figure 4. Resolution probabilities of MUSIC, L1-SVD, L1-EVD and L1-TEVD when snapshot number increases.

It is shown in Fig. 4 that the increase of the snapshots gains little improvement in the resolution ability of MUSIC, L1-TEVD performs the best, and L1-EVD also outperforms L1-SVD significantly. The result is identical to those shown in Figs. 1–3.

5. CONCLUSIONS

The problem of DOA estimation for highly correlated and coherent signals is addressed in this paper, and two methods, named L1-EVD and L1-TEVD, are proposed. Simulation results show that for highly correlated signals, L1-TEVD performs the best in both DOA estimation performance and computational efficiency among all the methods considered; when the signals are weakly correlated, L1-EVD performs better than L1-TEVD, and is just slightly worse than L1-SVD while saving about 20% computation time. If the additive noise is not Gaussian, i.e., impulsive [27] or Laplacian [28] the proposed method needs some modifications which will be researched in the future work.

APPENDIX A. PROOF OF LEMMA 1

The zero-mean and Gaussian properties of the incident signals and additive noise indicate that $\mathbf{x}(n)$ is also zero-mean and Gaussian, and $E(\mathbf{x}(n)\mathbf{x}^T(n)) = \mathbf{0}$, $E(\mathbf{x}(n)\mathbf{x}^H(n)) = \mathbf{R}$, thus

$$\begin{aligned}
 E(\tilde{\mathbf{R}}_{ik}\tilde{\mathbf{R}}_{lm}) &= E\left\{\left(\frac{1}{N}\sum_{n=1}^N\mathbf{x}_i(n)\mathbf{x}_k^H(n)-\mathbf{R}_{ik}\right)\left(\frac{1}{N}\sum_{n=1}^N\mathbf{x}_l(n)\mathbf{x}_m^H(n)-\mathbf{R}_{lm}\right)\right\} \\
 &= \frac{1}{N^2}E\left\{\sum_{n_1=1}^N\sum_{n_2=1}^N\mathbf{x}_i(n_1)\mathbf{x}_k^H(n_1)\mathbf{x}_l(n_2)\mathbf{x}_m^H(n_2)\right\}-\mathbf{R}_{ik}\mathbf{R}_{lm} \\
 &= \frac{1}{N^2}E\left\{\sum_{n=1}^N\mathbf{x}_i(n)\mathbf{x}_k^H(n)\mathbf{x}_l(n)\mathbf{x}_m^H(n)\right\} \\
 &\quad + \frac{1}{N^2}E\left\{\sum_{n_1=1}^N\sum_{\substack{n_2=1 \\ n_2\neq n_1}}^N\mathbf{x}_i(n_1)\mathbf{x}_k^H(n_1)\mathbf{x}_l(n_2)\mathbf{x}_m^H(n_2)\right\}-\mathbf{R}_{ik}\mathbf{R}_{lm} \\
 &= \frac{1}{N}(\mathbf{R}_{ik}\mathbf{R}_{lm}+\mathbf{R}_{im}\mathbf{R}_{lk})-\frac{1}{N}\mathbf{R}_{ik}\mathbf{R}_{lm} \\
 &= \frac{1}{N}\mathbf{R}_{im}\mathbf{R}_{lk}.
 \end{aligned}$$

REFERENCES

1. Liang, J. and D. Liu, "Two L-shaped array-based 2-D DOAs estimation in the presence of mutual coupling," *Progress In Electromagnetics Research*, Vol. 112, 273–298, 2011.
2. Yang, P., F. Yang, and Z.-P. Nie, "DOA estimation with sub-array divided technique and interpolated esprit algorithm on a cylindrical conformal array antenna," *Progress In Electromagnetics Research*, Vol. 103, 201–216, 2010.
3. Mukhopadhyay, M., B. K. Sarkar, and A. Chakraborty, "Augmentation of anti-jam GPS system using smart antenna with a simple DOA estimation algorithm," *Progress In Electromagnetics Research*, Vol. 67, 231–249, 2007.
4. Tu, T. C., C. M. Li, and C. C. Chiu, "The performance of polarization diversity schemes in outdoor micro cells," *Progress In Electromagnetics Research*, Vol. 55, 175–188, 2005.
5. Cheng, S. C. and K. C. Lee, "Reducing the array size for DOA estimation by an antenna mode switch technique," *Progress In Electromagnetics Research*, Vol. 131, 117–134, 2010.
6. Zaharis, Z. D., K. A. Gotsis, and J. N. Sahalos, "Adaptive beamforming with low side lobe level using neural networks trained by mutated Boolean PSO," *Progress In Electromagnetics Research*, Vol. 127, 139–154, 2012.
7. Liu, F., J. Wang, R. Du, L. Peng, and P. Chen, "A second-order cone programming approach for robust downlink beamforming with power control in cognitive radio networks," *Progress In Electromagnetics Research M*, Vol. 18, 221–231, 2011.
8. Mallipeddi, R., J. P. Lie, P. N. Suganthan, S. G. Razul, and C. M. S. See, "A differential evolution approach for robust adaptive beamforming based on joint estimation of look direction and array geometry," *Progress In Electromagnetics Research*, Vol. 119, 381–394, 2011.
9. Krim, H. and M. Viberg, "Two decades of array signal processing research: The parametric approach," *IEEE Signal Processing Mag.*, 67–94, Jul. 1996.
10. Si, W., L. Wan, L. Liu, and Z. Tian, "Fast estimation of frequency and 2-D DOAs for cylindrical conformal array antenna using state-space and propagator method," *Progress In Electromagnetics Research*, Vol. 137, 51–71, 2013.
11. Weiss, A. J. and B. Friedlander, "On the Cramer-Rao bound for direction finding of correlated signals," *IEEE Trans. Signal Processing*, Vol. 41, No. 1, 495–499, Jan. 1993.

12. Linebarger, D. A., R. D. DeGroat, and E. M. Dowling, "Efficient direction-finding methods employing forward/backward averaging," *IEEE Trans. Signal Processing*, Vol. 42, No. 8, 2136–2145, Aug. 1994.
13. Malioutov, D., "A sparse signal reconstruction perspective for source localization with sensor arrays," M. S. Thesis, MIT, Cambridge, MA, Jul. 2003.
14. Fuchs, J. J., "On the application of the global matched filter to DOA estimation with uniform circular arrays," *IEEE Trans. Signal Processing*, Vol. 49, No. 4, 702–709, Apr. 2001.
15. Malioutov, D., M. Cetin, and A. S. Willsky, "A sparse signal reconstruction perspective for source localization with sensor arrays," *IEEE Trans. Signal Processing*, Vol. 53, No. 8, 3010–3022, Aug. 2005.
16. Liu, F., L. Peng, M. Wei, and S. Guo, "An improved L1-SVD algorithm based on noise subspace for DOA estimation," *Progress In Electromagnetics Research C*, Vol. 29, 109–122, May 2012.
17. Hyder, M. M. and K. Mahata, "Direction-of-arrival estimation using a mixed L_{2,0} norm approximation," *IEEE Trans. Signal Processing*, Vol. 58, No. 9, 4646–4655, Sep. 2010.
18. Liu, Z. M., Z. T. Huang, and Y. Y. Zhou, "Direction-of-arrival estimation of wideband signals via covariance matrix sparse representation," *IEEE Trans. Signal Processing*, Vol. 59, No. 9, 4256–4270, Sep. 2011.
19. Zhang, Y., Q. Wan, and A.-M. Huang, "Localization of narrow band sources in the presence of mutual coupling via sparse solution finding," *Progress In Electromagnetics Research*, Vol. 86, 243–257, 2008.
20. Chen, S. S., D. L. Donoho, and M. A. Saunders, "Atomic decomposition by basis pursuit," *SIAM Review*, Vol. 43, No. 1, 129–159, 2001.
21. Berg, E. and M. P. Friedlander, "In pursuit of a root," *Technique Report, University of British Columbia*, BC, Canada, Tech. Rep. TR-2007-19, 1–8, 2007.
22. Hansen, P. C., "Analysis of discrete ill-posed problems by means of the L-curve," *SIAM Review*, Vol. 34, No. 4, 561–580, 1992.
23. Natarajan, B. K., "Sparse approximate solutions to linear systems," *SIAM J. Comput.*, Vol. 24, 227–234, 1995.
24. Kaveh, M. and A. J. Barabell, "The statistical performance of the MUSIC and the minimum-norm algorithms in resolving plane waves in noise," *IEEE Transactions on Acoustics, Speech, and*

- Signal Processing*, Vol. 34, No. 2, 331–341, Apr. 1986.
25. Brillinger, D. R., *Time Series: Data Analysis and Theory*, SIAM Press, 2001.
 26. Tropp, J. A. and S. J. Wright, “Computational methods for sparse solution of linear inverse problems,” *Proceedings of the IEEE*, Vol. 98, No. 6, 948–958, Jun. 2010.
 27. Zhang, Y., Q. Wan, H. P. Zhao, and W. L. Yang, “Support vector regression for basis selection in Laplacian noise environment,” *IEEE Signal Processing Letters*, Vol. 14, No. 11, 871–874, Nov. 2007.
 28. Zhang, Y., H. Zhao, and Q. Wan, “Single snapshot 2D-DOA estimation in impulsive noise environment using linear arrays,” *ACES Journal*, Vol. 27, No. 12, 991–998, Dec. 2012.